TRANSPORT OF MACROPHAGE Fc RECEPTORS AND Fc RECEPTOR-BOUND LIGANDS TO LYSOSOMES

By PENTTI UKKONEN, VICTORIA LEWIS, MARK MARSH, ARI HELENIUS, AND IRA MELLMAN

From the Department of Cell Biology, Yale University School of Medicine, New Haven, Connecticut 06510

Mouse macrophages express several distinct plasma membrane receptors for the Fc domain of IgG (1). The most numerous and best characterized is the trypsin-resistant Fc receptor (FcR)[1] specific for IgG1 and IgG2b. The receptor is a 60-kD transmembrane glycoprotein (2, 3) involved in a variety of macrophage host defense functions, such as the release of potent cytotoxic and inflammatory agents, the pinocytosis of soluble immune complexes, and the phagocytosis of large IgG-coated particles (1).

Previous studies of FcR-mediated endocytosis have shown that certain ligands can modulate the cell surface expression of the receptor (4–6). Internalization of soluble or particulate IgG-containing immune complexes is accompanied by the net loss of FcR from the cell surface. Both receptor and ligand are degraded, presumably in lysosomes, and *de novo* synthesis is required to restore the original number of surface FcR (6). On the other hand, when the ligand is a monovalent Fab fragment of the antireceptor antibody 2.4G2 (7), FcR-Fab complexes rapidly recycle between the cell surface and a nonlysosomal endocytic compartment, i.e., endosomes (5). There is no decrease in the number of surface receptors and no acceleration in the rate of receptor degradation.

Many basic questions remain unanswered regarding the control of FcR-mediated endocytosis in macrophages. The pathways and organelles involved in the uptake of receptor-ligand complexes have been only superficially characterized (8), and the intracellular fate of the receptor during IgG complex uptake has yet to be directly shown. In addition, the mechanism by which the multivalent antibody-antigen complexes prevent FcR recycling, in contrast to the behavior of the monovalent antireceptor Fab, is of particular interest. While the different valencies of these two ligands have been suggested to play a role (6), it is clear

P. Ukkonen was a recipient of a fellowship from the Fogarty International Center, National Institutes of Health, Bethesda, MD, and was also supported by grants from the Finnish Cultural Foundation and Virustautien Tutkimuksen Kannatusyhdistys; M. Marsh was a recipient of an award from the Swebilius Fund. This work was supported by research grants AI-18582 and AI-18599 to A. Helenius from the National Institutes of Health, and NIH grants GM-29765 and GM-33904 to I. Mellman. V. Lewis was supported by an NIH predoctoral training grant. Address correspondence to I. Mellman, Department of Cell Biology, Yale University School of Medicine, New Haven, CT 06510. P. Ukkonen's present address is Department of Virology, University of Helsinki, Haartmanikatu 3, 00290 Helsinki 29, Finland. M. Marsh's present address is Institute for Cancer Research, Chester Beatty Laboratories, Fulham Road, London SW3 6JB, England.

[1] *Abbreviations used in this paper:* DNP-BSA, DNP-modified BSA; FcR, Fc receptor.

 J. Exp. Med. © The Rockefeller University Press · 0022-1007/86/04/0952/20 $1.00
Volume 163 April 1986 952–971

that IgG complexes and anti-FcR Fab also differ in their modes of attachment to the receptor. Conceivably, the signal that results in FcR degradation and down regulation is provided by the binding of intact Fc domains rather than by the aggregation of adjacent receptors by multivalent ligands. In this paper, we characterize the internalization and intracellular fate of FcR bound to either IgG complexes or multivalent preparations of 2.4G2 Fab in the J774 macrophage cell line using both biochemical and morphological techniques. We show that multivalent FcR-bound ligands are taken up via coated pits, coated vesicles, and endosomes, and result in the delivery of both receptor and ligand to lysosomes. Since multivalent Fab preparations were as effective as IgG-containing immune complexes at mediating lysosomal transport, these data support the concept that ligand valency, and not the presence of intact Fc domains, is an important determinant of FcR transport during receptor-mediated endocytosis.

Materials and Methods

Cells and Cell Culture. The mouse macrophage-like cell line, J774, was maintained in suspension culture as described previously (5). For experiments, cells were plated on 10-cm tissue culture dishes (10^7 cells per dish) or on 16-mm wells (5×10^5 cells per well) for 1 h at 37°C in alpha-modified Eagle's medium containing 8% FCS and 10 mM Hepes buffer at pH 7.4.

Antibodies and Antibody-Antigen Complexes. Affinity purified rabbit anti-DNP IgG was prepared as described (9). Immune complexes were formed just before use by incubating anti-DNP IgG (20 μg/ml) with DNP-modified BSA (DNP-BSA; >12 DNP groups/BSA molecule) (9) at an IgG/BSA molar ratio of 2.5:1 (6). Incubations were performed at 37°C or at room temperature for 30–60 min. The monoclonal rat anti–mouse FcR antibody, designated 2.4G2, was grown as ascites and purified as described (2, 7). Fab fragments 2.4G2 were prepared by papain digestion and purified by DEAE-cellulose chromatography and Sephadex G-50 (Pharmacia Fine Chemicals, Piscataway, NJ) gel filtration (7). The antibody preparations were analyzed by SDS-PAGE and by HPLC using an Ultro-Pac TSK-G 3000-SW column (LKB, Bromma, Sweden) and found to be homogeneous. Anti-DNP IgG, DNP-BSA, and 2.4G2 Fab were labeled with $Na^{125}I$ (10 mCi/ml, 0.5 mCi/50 μg protein; Amersham Corp., Arlington Heights, IL) using Iodogen (Pierce Chemical Co., Chicago, IL) as described (4). Monospecific rabbit anti–FcR antisera, produced against purified, SDS-denatured receptor, was used for immunoprecipitation without purification. These antisera detect free receptor and receptor-ligand complexes with equal efficiency (4, 6).

Preparation of Colloidal Gold Conjugates. Colloidal gold was prepared by sonication under conditions that generated particles 5–10 nm in diameter (10). Stable gold conjugates of DNP-BSA and 2.4G2 Fab were made by incubating 1 mg of either protein (containing trace amounts of ^{125}I) with 18 ml of colloidal gold for 3 min at room temperature. The reaction was stopped with 2 ml of 1% PEG 20,000. The gold particles were pelleted by centrifugation in an SW 40 rotor at 39,000 rpm for 1 h at 4°C. The pellet was resuspended in 0.2% PEG in PBS and centrifuged again. The final pellet was resuspended in 0.5 ml of 0.2% PEG in PBS containing 0.02% NaN_3. The concentration of BSA or Fab was calculated from the recovered radioactivity. Both gold conjugates were judged by electron microscopy to be monodisperse and remained stable for several weeks at 4°C. For some experiments, DNP-BSA-gold and Fab-gold conjugates were radioiodinated after their formation using Iodogen (4).

Colloidal gold–labeled immune complexes for electron microscopy were formed exactly as described above for the unconjugated immune complexes, except that DNA-BSA-gold was used in place of DNP-BSA.

Binding and Internalization Assays. To distinguish between cell surface-bound and internalized IgG/DNP-BSA complexes, cell monolayers incubated with ^{125}I-IgG/DNP-

BSA were treated with 1 mg/ml subtilisin (Sigma Chemical Co., St. Louis, MO) for 2 h at 4°C, conditions that remove 80–90% of surface-bound complexes (6). In experiments designed to measure the degradation of internalized ligand, immune complexes were prepared using ^{125}I-DNP-BSA since IgG is relatively resistant to lysosomal proteolysis (6).

Cell Fractionation. After incubation in the appropriate ligand, cell monolayers were washed with cold PBS, harvested by scraping, and combined with 10^8 unlabeled J774 cells obtained from suspension culture. Homogenates were prepared using a stainless steel Dounce homogenizer (Kontes Co., Vineland, NJ), the homogenate centrifuged at 750 *g* for 10 min at 4°C, and the postnuclear supernatant centrifuged in 27% Percoll as described (11). Centrifugation was performed using Quick-Seal tubes (Beckman Instruments, Inc., Palo Alto, CA) in either a Beckman 70 Ti rotor (2 h, 16,000 rpm) or a Beckman VTi50 rotor (1 h, 18,000 rpm). 1-ml fractions were collected, and ^{125}I determined using a Beckman gamma counter. β-Glucuronidase and horseradish peroxidase activities were measured spectrophotometrically in the presence of 0.1% Triton X-100 (11).

Immunoprecipitation. J774 cells were plated in 35-mm dishes (10^6 cells per dish) and radioiodinated at 4°C using lactoperoxidase and glucose oxidase (12). Labeled cells were then incubated at 37°C in complete medium in the presence or absence of saturating concentrations of IgG/DNP-BSA immune complexes (20 μg/ml) (6) or 2.4G2 Fab (either free or colloidal gold–conjugated, 3–5 μg/ml) (2). After 1–2 h, monolayers were washed with cold PBS, harvested by scraping, and collected by centrifugation (750 *g*, 4°C). Cell pellets were combined with 10^7 unlabeled cells, homogenized, and fractionated by centrifugation in Percoll density gradients as above. 1-ml fractions were collected and lysed at 4°C in PBS containing 0.5% Triton X-100, 1 mM PMSF, 10 mM leupeptin, and aprotinin (13). FcR was immunoprecipitated as described previously using conditions that were optimized to ensure >80% recovery of ^{125}I-FcR (3). Briefly, 2 μl of a rabbit anti-FcR antiserum was added per 1-ml fraction (4°C, 1 h) followed by 10 μl of affinity-purified goat anti-rabbit IgG (Boehringer Mannheim Diagnostics, Inc., Houston, TX) (final concentration 10 μg/ml, 4°C, 1 h). Immune complexes were collected using fixed *Staphyloccocus aureus* (Zymed Laboratories, So. San Francisco, CA). ^{125}I-FcR was stripped from the immunoadsorbant in electrophoresis sample buffer containing 2% SDS (100°C, 5 min), *S. aureus* removed by centrifugation, and the supernatant applied to SDS-polyacrylamide minigels (4–11% acrylamide gradients). After electrophoresis, gels were dried, autoradiographed, and the radioactive bands cut out for quantitation (13).

Electron Microscopy. J774 cells were plated on 16-mm wells as confluent monolayers 2–3 h before use. The cells were incubated with gold-labeled ligands in 0.2 ml of complete medium at 37°, 17°, or 4°C for various times. For some experiments, incubations were performed in the presence of 100 or 200 μg/ml of 2.4G2 IgG (or Fab) to block binding to FcR. After extensive washing with cold PBS, monolayers were fixed with 2.5% glutaraldehyde in 0.05 M sodium cacodylate buffer (pH 7.4, 30 min), postfixed in 2% OsO_4 (2 h, 4°C), and block-stained with 0.5% uranyl acetate. Samples were then dehydrated with ethanol and embedded in Epon. Sections were stained with uranyl acetate and lead citrate, and examined with a JEM-100CX electron microscope (JEOL USA, Peabody, MA).

Results

Pathway of FcR-mediated Endocytosis. For electron microscopic identification of the organelles involved in FcR-mediated endocytosis, a soluble immune complex containing colloidal gold was used. DNP-BSA was first adsorbed to 5–10-nm colloidal gold particles. Affinity-purified anti-DNP IgG was then added (2.5:1 IgG/BSA molar ratio) to yield IgG/DNP-BSA immune complexes on the surface of the gold particles. Prepared in this way, the resulting gold-labeled IgG complexes closely resembled the receptor's physiological ligand (6).

Using conjugates prepared with ^{125}I-anti-DNP IgG or ^{125}I-DNP-BSA, gold-

labeled immune complexes were shown to bind specifically to FcR on J774 cells. First, monolayers were incubated with saturating concentrations of the conjugate (20 μg/ml IgG) for 2 h at 4°C in the presence or absence of excess 2.4G2, an antireceptor mAb that selectively blocks the binding of immune complexes to FcR (2, 6). Binding of both ^{125}I-IgG/DNP-BSA-gold and IgG/^{125}I-DNP-BSA-gold was >90% inhibited by either 2.4G2 IgG or Fab (100 μg/ml). This inhibition was confirmed by electron microscopy: the number of gold particles observed on the plasma membrane of cells exposed to IgG/DNP-BSA-gold at 4°C was reduced 10-fold by simultaneous incubation with 100 μg/ml 2.4G2 IgG. In addition, ~10^6 molecules of IgG bound per J774 cell irrespective of whether the anti-DNP IgG had been complexed with DNP-BSA-gold or free DNP-BSA, indicating that the presence of colloidal gold did not greatly affect the attachment properties of immune complexes. Finally, J774 cells did not accumulate free ^{125}I-DNP-BSA-gold (i.e., DNP-BSA-gold not complexed with anti-DNP IgG) even after 2 h at 4° or 37°C, indicated both by measuring cell-associated radioactivity and by electron microscopy. Thus, the colloidal gold preparations used in these studies did not adsorb nonspecifically to the J774 cell plasma membrane.

When viewed in thin sections by electron microscopy, gold-labeled complexes bound to J774 cells at 4°C were seen on the plasma membrane often in small clusters and only occasionally at coated pits. After 5 min at 37°C, however, they were distributed mainly in coated pits, coated vesicles, and in peripheral tubules and vesicles characteristic of endosomes (Fig. 1, *A–D*, see also Fig. 7*A*). After 15 min, the majority of the gold was found in larger endosomal vacuoles located in both the peripheral and perinuclear cytoplasm (Fig. 1, *E* and *F*, see also Fig. 7*A*). The gold was always closely associated with either the limiting membrane of these endosomes or, more frequently, with the surfaces of their membrane inclusions. IgG-gold was only occasionally seen in dense, lysosome-like vesicles at early time points. After 1 h, however, most of the gold was found in condensed multivesicular bodies and electron dense lysosomes where it was no longer preferentially associated with membranes (Fig. 1, *G* and *H*). J774 cell lysosomes are easily identified by their electron-dense contents and characteristic membranous inclusions.

The morphological data showed that the internalization of multivalent FcR-bound ligands proceeded via the standard pathway described for a variety of other plasma membrane receptors: passage through coated pits, coated vesicles, peripheral and perinuclear endosomes, and finally lysosomes (14–16). The data also suggested that IgG complexes, as previously shown for epidermal growth factor (17), were concentrated on the internal membrane inclusions of multivesicular endosomes and that they remained largely membrane-bound until the point of delivery to lysosomes.

Subcellular Localization of IgG Complexes. To follow the transport of FcR bound ligands by cell fractionation, ^{125}I-IgG/DNP-BSA complexes were used without the colloidal gold label (6). J774 cells were first incubated with saturating concentrations of ligand (20 μg/ml IgG) in the cold or at 37°C for varying lengths of time, whereafter the monolayers were washed, homogenized, and centrifuged in Percoll density gradients. As shown in Fig. 2*A*, ^{125}I-IgG complexes that were bound to the plasma membrane at 4°C, sedimented as a symmetrical

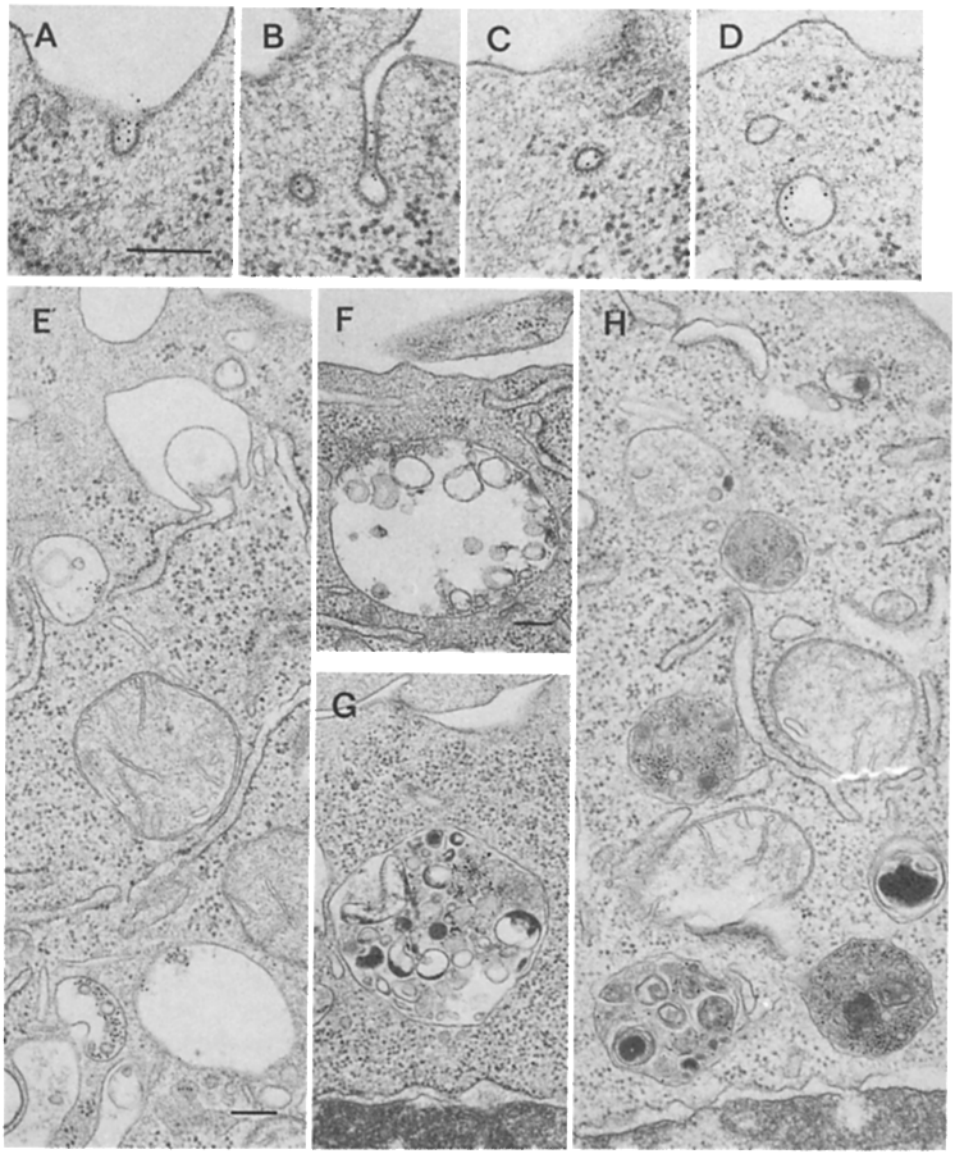

FIGURE 1. Electron microscopic localization of IgG/DNP-BSA-gold internalized at 37°C. J774 cell monolayers were incubated with IgG/DNP-BSA gold (20 μg IgG/ml; 5 nm gold) for various times at 37°C. After 5 min incubation, the gold particles were seen in coated pits (*A*), which were often deeply invaginated (*B*), coated vesicles (*B*, *C*), and in small peripheral endosomes (*D*). Within 15 min, the complexes were found in peripheral and perinuclear endosomes, many of which contained internal vesicles (*E*). After 60 min, the marker was localized in larger multivesicular bodies (*F*), more condensed multivesicular structures (*G*), and in mature, dense lysosomes (*H*). In multivesicular bodies (*E*, *F*), the gold was typically located on the membrane of the small inner vesicles, while in the more condensed multivesicular bodies (*G*) and electron-dense lysosomes (*H*) the gold particles were apparently free in the matrix. Bar, 0.2 μm.

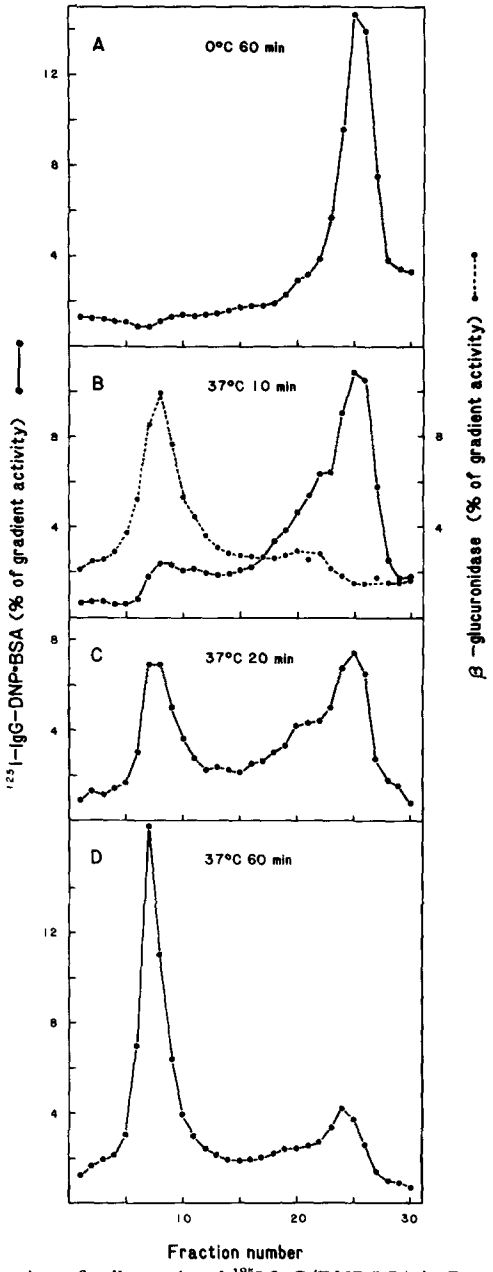

FIGURE 2. Sedimentation of cell-associated ^{125}I-IgG/DNP-BSA in Percoll density gradients. Confluent 10-cm dishes of J774 cells (10^7 cells/dish) were incubated with ^{125}I-IgG/DNP-BSA at 0°C for 60 min (*A*), or at 37°C for 10 min (*B*), 20 min (*C*), or 60 min (*D*). The cells were then washed, harvested by scraping, combined with 10^8 unlabeled cells, and homogenized. The postnuclear supernatants were centrifuged in 27% Percoll density gradients (I I). Fractions were collected from the bottom of the tube, ^{125}I determined, and lysosomes localized using β-glucuronidase as the marker enzyme (broken line in *B*). Surface-bound ^{125}I-IgG complexes sedimented as a sharp light density peak (ρ = 1.03 g/ml) near the top of the gradient (*A*). Following internalization at 37°C, the complexes shifted progressively to the high density lysosomal fractions (ρ = 1.09 g/ml) (*B–D*). 3–6 × 10^4 cpm of ^{125}I were applied to each gradient.

low density peak (ρ = 1.03 g/ml) near the top of the gradient. After 10 min at 37°C, however, ~10% of the radioactivity was found in high density fractions cosedimenting with the lysosomal marker enzyme β-glucuronidase (Fig. 2*B*). The low density peak had also become broader and asymmetric, exhibiting a shoulder of intermediate density. Since at this time point >40% of cell-associated IgG complexes were intracellular (i.e., resistant to removal by subtilisin) (6), the shoulder was likely to reflect the presence of internalized ligand in endosomes known to sediment as a broad band of low to intermediate density (11). After 20 min, at which time approximately two-thirds of the ligand was intracellular, the gradient radioactivity was evenly divided between the low to intermediate density peak and the high density lysosomal peak (Fig. 2*C*). By 1 h, >70% of the internalized ^{125}I-IgG complexes had been transferred to lysosomes (Fig. 2*D*). The kinetics of appearance of ligand in high density fractions are in agreement with the finding that degradation of IgG/^{125}I-DNP-BSA complexes can be detected within 5–10 min after internalization (6), as well as with the electron microscopy that showed that most of the internalized IgG complexes were found in lysosomes only after 1 h of uptake (Fig. 1).

Transport of Monomeric and Aggregated Anti–FcR Antibody. Previous work has shown that a monovalent FcR-bound ligand, such as a Fab fragment of the antireceptor mAb 2.4G2, is poorly transported to lysosomes (5). ^{125}I-Fab binds efficiently to the receptor and is delivered to endosomes, but instead of continuing to lysosomes it is recycled back to the cell surface still bound to FcR. Although it seems likely that the different fates of the monovalent Fab and the multivalent immune complexes are due to their different valencies, the two ligands also differ in how they bind to FcR, Fab via its antigen combining site and IgG complexes via the Fc domains of intact IgG molecules. To test whether the signal for transport to lysosomes depends on ligand valency or on mode of attachment to the receptor, we examined the endocytosis of multivalent complexes of ^{125}I-2.4G2 Fab.

Multivalent Fab complexes were prepared by adsorption of the monovalent antibody fragments to colloidal gold particles. While the precise valency of the resulting conjugates could not be accurately determined, we estimate that between 2 and 12 molecules of Fab adsorbed to individual gold particles which in these preparations varied in diameter from 5 to 10 nm. These figures were obtained from more accurate measurements using *S. aureus* protein A, a protein with a Stokes radius similar to an IgG Fab fragment (18) (H. Geuze, personal communication). The ^{125}I-Fab-gold conjugate bound specifically to FcR, since binding to J774 cells (1 h, 4°C) could be inhibited up to 85% by simultaneous incubation with an excess of unconjugated 2.4G2 Fab or 2.4G2 IgG (200 μg/ml). Unlike unconjugated Fab, however, the Fab-gold could not be dissociated from the receptor by acidic pH (pH < 4.3) (5).

Cells were incubated with ^{125}I-Fab or ^{125}I-Fab-gold for 1 h at 4°C or 37°C, homogenized, and centrifuged in Percoll density gradients. As shown in Fig. 3*A*, ^{125}I-Fab-gold bound in the cold sedimented as a single low density peak corresponding to the plasma membrane. After 1 h at 37°C, however, most of the radioactivity was found in the high density region of the gradient, cosedimenting with the lysosomal marker enzyme β-glucuronidase (Fig. 3*B*). In contrast, uncon-

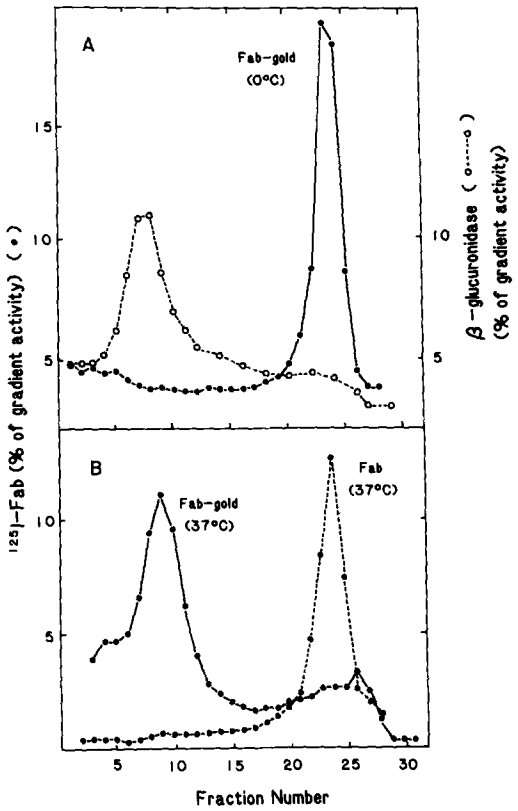

FIGURE 3. Sedimentation of cell-associated ^{125}I-2.4G2 Fab and ^{125}I-Fab-gold conjugates in Percoll density gradients. Confluent 6-cm dishes of J774 cells were incubated in complete medium containing ^{125}I-Fab or ^{125}I-Fab-gold (3–5 μg Fab/ml) for 60 min at either 0°C or 37°C. Monolayers were then washed with cold PBS, harvested by scraping, homogenized, and centrifuged in Percoll as in Fig. 2. (*A*) Sedimentation of ^{125}I-Fab-gold bound to cells at 0°C (–●–) and of the lysosomal marker enzyme β-glucuronidase (––○––). (*B*) The sedimentation of ^{125}I-Fab-gold (–●–) and unconjugated ^{125}I-Fab (––●––) after incubation with J774 cells at 37°C. Profiles shown were taken from different gradients, except that β-glucuronidase activity was determined from the 37°C ^{125}I-Fab-gold gradient. The amounts of radioactivity applied to each gradient were: ^{125}I-Fab-gold 37°C, 0.8×10^5 cpm; ^{125}I-Fab-gold 0°C, 0.4×10^5 cpm; unconjugated ^{125}I-Fab, 1.9×10^5 cpm. 80–90% of the radioactivity was recovered from each gradient.

jugated ^{125}I-Fab sedimented predominantly in the low density plasma membrane-endosome region of the gradient (Fig. 3*B*). Since no attempt was made to remove surface-bound ^{125}I-Fab by treatment with pH 4 medium, the fraction of cell-associated unconjugated Fab (15%) which was in endosomes after 1 h at 37°C could not be distinguished from plasma membrane-bound ^{125}I-Fab, which also sediments as a low density peak on Percoll gradients (5). Nevertheless, these data show that unlike the monomeric Fab, the gold conjugate was internalized and transported to lysosomes in a manner similar to authentic multivalent IgG immune complexes.

This conclusion was supported by electron microscopic examination of J774 cells exposed to Fab-gold for 5–60 min at 37°C. As shown in Fig. 4, gold particles

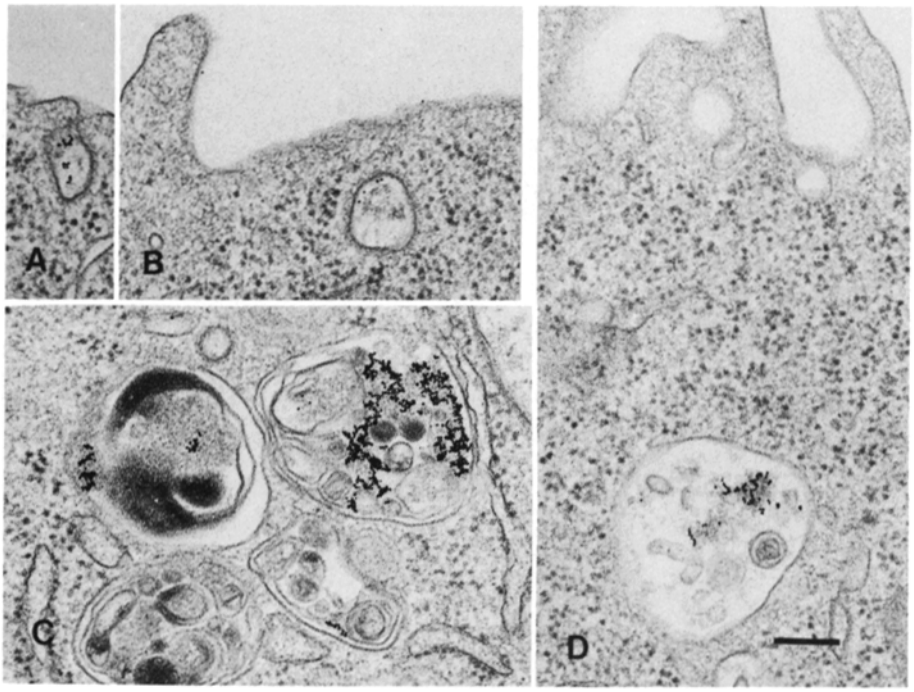

FIGURE 4. Localization of internalized 2.4G2 Fab-gold conjugates by electron microscopy. J774 monolayers were incubated with 2.4G2 Fab conjugated to 5–10-nm diameter particles of colloidal gold (Fab concentration 5 μg/ml). The general features of the uptake pathway were found to be similar to the uptake of IgG/DNP-BSA immune complexes (Fig. 1). After 5 min at 37°C, Fab-gold was found in clathrin coated pits (*A*), coated vesicles (*B*), as well as in multivesicular endosomes (*D*). By 1 h, almost all cell-associated gold was localized in electron dense lysosomes (*C*), in agreement with the Percoll gradient data (Fig. 3). The number of surface-bound and intracellular gold particles was decreased by 75–80% in cells incubated simultaneously with Fab-gold and 100 μg/ml unconjugated 2.4G2 IgG. Bar, 0.2 μm.

were seen in coated pits, coated vesicles, endosomes, and electron-dense lysosomes as already illustrated for gold-labeled IgG/DNP-BSA immune complexes in Fig. 1. Endocytosis was judged to be FcR-mediated since incubation with Fab-gold for 1 h at 37°C in the presence of 100 μg/ml unconjugated 2.4G2 reduced the number of cell-associated gold particles by 75%.

Taken together, these results give additional support to the suggestion that ligand valency, rather than the mode of attachment, determines the intracellular fate of FcR-bound ligands.

Transport of FcR to Lysosomes. To confirm that the uptake of multivalent (but not monovalent) ligands correlates with the transport of FcR to lysosomes, the subcellular localization of the receptor in cells exposed to various ligands was determined by Percoll gradient centrifugation and immunoprecipitation. J774 cells were surface iodinated in the cold and then incubated at 37°C for 0–2 h in the presence of Fab, Fab-gold, or IgG complexes. In some experiments, trace-iodinated Fab was used to monitor ligand distribution. After centrifugation in Percoll, ^{125}I-FcR was immunoprecipitated from each fraction using a rabbit antireceptor antibody. Immunoprecipitates were analyzed by SDS-PAGE and the

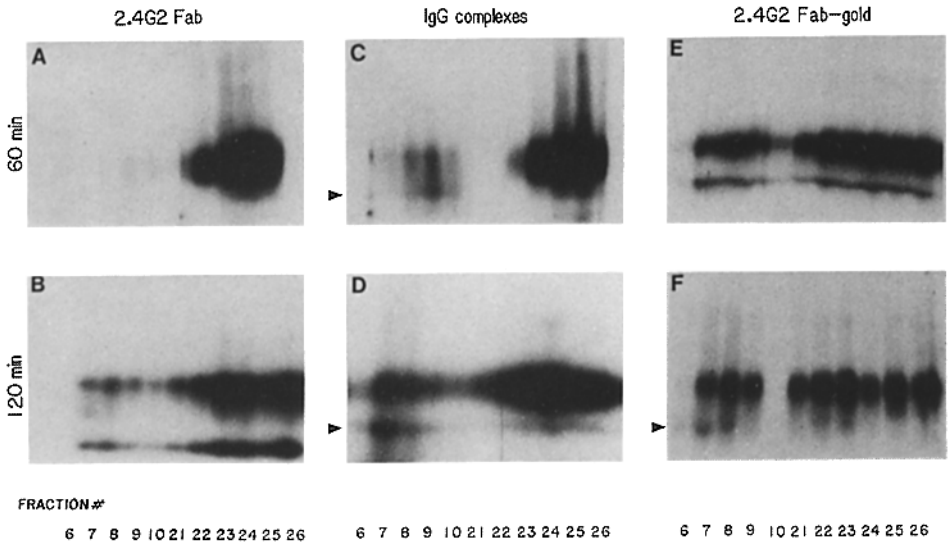

FIGURE 5. Immunoprecipitation of ^{125}I-labeled Fc receptor from Percoll gradient fractions. Monolayers of radioiodinated J774 cells in 6-cm plates were incubated in complete medium containing 2.4G2 Fab (3–5 μg/ml), IgG/DNP-BSA complexes (20 μg IgG/ml), or Fab-gold (3–5 μg/ml) for 60 or 120 min at 37°C. Cells were then harvested, homogenized, and centrifuged in 27% Percoll. Individual fractions were solubilized in buffer containing 0.5% Triton X-100 and ^{125}I-FcR detected using a rabbit anti–FcR antibody. Immunoprecipitates were analyzed by SDS-PAGE and autoradiographed. The lysosomes sedimented in fractions 6–10, which contained the major peak of β-glucuronidase activity (Figs. 2 and 3). Fractions 21–26 contained the plasma membrane/endosome region of the gradient. Labeled FcR electrophoresed as a broad 60-kD band (2, 3). Arrowheads indicate a presumptive 30-kD digestion intermediate of the receptor, which was detected only in the lysosomal fractions. The additional labeled low molecular mass (25–30 kD) bands in panels *B* and *E* represent ^{125}I-Fab tracer which was added in some experiments. Receptor-bound Fab is coprecipitated by the rabbit anti–FcR antibody under these conditions (11). These data are quantitated in Table I.

radioactive bands excised from dried gels and quantitated. The results of these experiments are shown in Fig. 5 and Table I.

The amount of labeled 60-kD FcR precipitated from the lysosomal region of the gradient (fractions 6–10) was significantly greater for cells incubated with IgG complexes (Fig. 5, *C* and *D*) or Fab-gold (Fig. 5, *E* and *F*) than for cells incubated with monovalent Fab (Fig. 5, *A* and *B*). When expressed as a percentage of the total amount of ^{125}I-FcR detected in each gradient, the fraction of receptor that cosedimented with lysosomes in cells exposed for 60 min to 2.4G2 Fab was only 4%, while in cells exposed to either of the multivalent ligands, ^{125}I-FcR in the lysosomal fractions accounted for ~25% of total (Table I). The amount of ^{125}I-FcR in the high density fractions increased slightly between 60 and 120 min (to 13% for Fab-treated cells and to 27–31% for IgG complex of Fab-gold-treated cells) (Table I).

Although multivalent ligands clearly increased the fraction of ^{125}I-FcR present in lysosomes, it was always exceeded by the amount of receptor precipitated from the low density endosome/plasma membrane fractions (fractions 21–26) (Table I), suggesting that not all surface FcR had been transported to lysosomes. However, this finding might also reflect the selective loss of immunoprecipitable

TABLE I

Distribution of ^{125}I-FcR After Percoll Gradient Centrifugation

Time of incubation	Gradient fractions	Ligand used during incubation		
		2.4G2 Fab	Fab-gold	IgG complexes
h		%	%	%
1	6–10	4.0	25.6	24.8
	21–26	96.0	74.4	75.2
2	6–10	13.2	31.2	27.0
	21–26	86.8	68.8	73.0

Monolayers of J774 cells in 6-cm plates were radioiodinated at 4°C using lactoperoxidase and glucose oxidase. Cultures were then fed with warm complete medium containing 2.4G2 Fab (3–5 μg/ml), Fab-gold (3–5 μg/ml), or IgG/DNP-BSA complexes (20 μg/ml) and incubated for 1 or 2 h at 37°C. Cells were washed with cold PBS, harvested by scraping, homogenized, and centrifuged in Percoll density gradients. ^{125}I-FcR was immunoprecipitated from individual detergent-solubilized gradient fractions and displayed on SDS-polyacrylamide gels (Fig. 5). Using autoradiographs of dried gels as templates, the radioactive bands (including the presumptive 30-kD digestion intermediate; see Fig. 5) were cut out and quantified. The amounts of ^{125}I-FcR immunoprecipitated from the lysosomal region (fractions 6–10) and the endosome/plasma membrane region (fractions 21–26) of the gradients were expressed as percentage of the total amount of labeled FcR recovered from each gradient.

FcR from the lysosomal fractions due to receptor degradation. That such degradation occurred is supported by previous studies that documented a greatly increased rate of FcR turnover in cells exposed to IgG complexes (6). In addition, immunoprecipitation of ^{125}I-FcR from the high density fractions often yielded a presumptive 30-kD digestion intermediate corresponding to the transmembrane and cytoplasmic domains of the 60-kd receptor (3) (Fig. 5, arrows). Since IgG complexes accelerate the halftime for FcR degradation from >15 h to 4–5 h (6), we estimate that after 2 h, ~25% of the FcR would be lost due to degradation. Thus, the total amount of labeled receptor either degraded or present in lysosomes after 2 h in multivalent ligand could account for up to 55% of the initial amount of surface receptor, in general agreement with the percentage of surface FcR lost (65%) after 2 h incubation in IgG complexes (6). Exposure of cells to monovalent 2.4G2 Fab did not detectably increase the rate of ^{125}I-FcR degradation relative to controls (unpublished results).

Effect of NH_4Cl, Monensin, and Intermediate Temperature on FcR-mediated Transport to Lysosomes. The binding of IgG complexes to FcR is relatively insensitive to low pH; <25% of the ligand dissociates from cell surface FcR during a 2-h incubation at 0°C, whether at neutral or acidic pH (pH 3.0–5.5) (6). Thus, unlike many ligands whose delivery to lysosomes is blocked by agents that elevate intravesicular pH (e.g., NH_4Cl and monensin) (19, 20), the interaction between IgG-complexes and FcR should not itself be altered by treatment with such agents.

To determine the role of acidic pH in endosomes and lysosomes on the transport of FcR-bound ligands, J774 cells were treated with 10 mM NH_4Cl or

20 μM monensin for 30–60 min at 37°C before the addition of ^{125}I complexes (21). After 90 min at 37°C, the cells were homogenized and centrifuged in Percoll density gradients. As shown in Fig. 6, neither inhibitor prevented the transfer of the ^{125}I-IgG complexes to high density lysosomes. Although the low density peaks containing endosomes and the plasma membrane were somewhat larger and broader than in the control gradient, subtilisin treatment of intact cells at 4°C indicated that the percentage of ^{125}I-IgG complexes remaining on the cell surface was not affected by either drug; after 90 min at 37°C in the presence or absence of inhibitors, only 20% of the cell-associated radiolabel was accessible to removal by subtilisin. Based on the distribution of ^{125}I-IgG complexes in the Percoll gradient fractions (Fig. 6, *A–C*), it could be calculated that the percentage of radiolabel in endosomes was increased in monensin- and NH_4Cl-treated cells relative to control cells (35% vs. 20%) (Table II). These results indicate that the transport of FcR-bound ligands from endosomes to lysosomes does not depend absolutely on low intravesicular pH. Similarly, NH_4Cl did not inhibit the transport to lysosomes of a marker of fluid phase endocytosis, horseradish peroxidase (not shown).

The only effective inhibitor of IgG complex transport to lysosomes was incubation at 17°C. As shown in Fig. 6*D*, Percoll gradient centrifugation showed that little or no ligand reached the high density lysosomal fractions even after 90 min at 17°C. ~50% of the cell-associated radiolabel was intracellular (resistant to removal by subtilisin) at this time point. Even after 4 h at 17°C, no IgG complex degradation was detected as TCA-soluble radiolabel in the medium, using either ^{125}I-IgG/DNP-BSA or IgG/^{125}I-DNP-BSA as ligand.

To characterize the 17°C block further, cells exposed to colloidal gold–conjugated IgG complexes were examined by electron microscopy. After 1 h at the intermediate temperature, gold particles were found in electron lucent vesicular and tubular endosomes usually in the peripheral cytoplasm. In contrast to the results obtained at 37°C (Fig. 1), IgG-gold internalized at 17°C was rarely observed in multivesicular endosomes. Moreover, when present in these structures, the marker was usually associated with the endosome's limiting membrane rather than with the small internal vesicles as found in control cells and in cells treated with NH_4Cl or monensin. Fig. 7 compares multivesicular endosomes containing IgG-gold which had been internalized at either 37°C (Fig. 7*A*) or 17°C (Fig. 7*B*) to illustrate the different distributions of the marker under conditions that permit or block ligand transport to lysosomes, respectively.

Discussion

The results presented here clarify several issues concerning the control of FcR traffic and cell surface expression during receptor-mediated endocytosis in J774 cells. The most important of these regards the mechanism of FcR down-regulation and the principles underlying molecular sorting in endosomes. When taken together with previous reports (5, 6), the present data show that ligand valency is a key factor in determining whether internalized FcR are recycled back to the plasma membrane or are transported to lysosomes and degraded. We have found that FcR can mediate the endocytosis of both monovalent and multivalent ligands (monoclonal antireceptor Fab fragments and Fab-gold or IgG immune com-

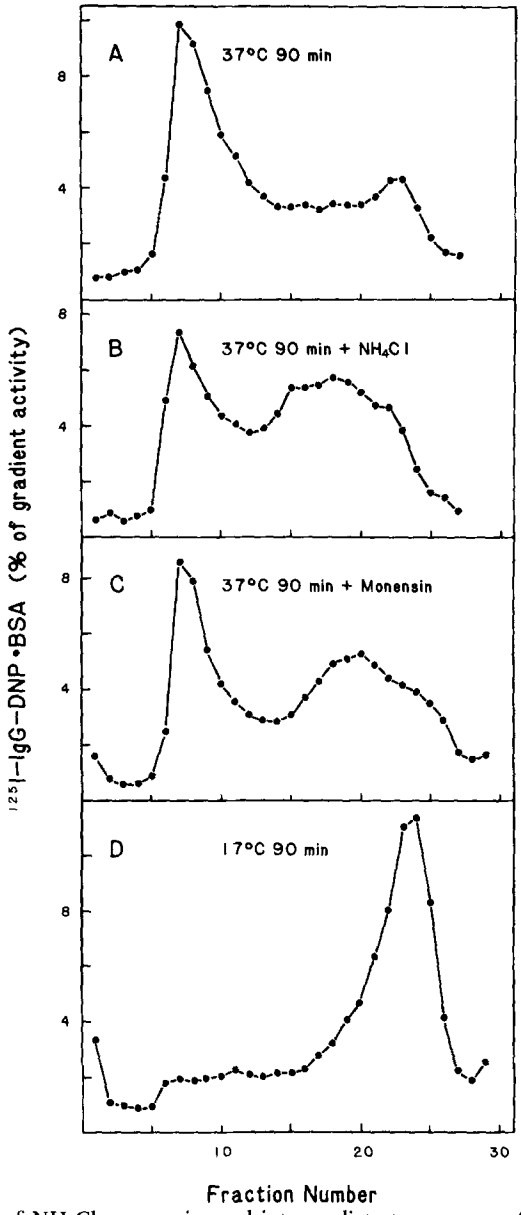

FIGURE 6. Effect of NH_4Cl, monensin, and intermediate temperature (17°C) on the sedimentation of cell-associated ^{125}I-IgG/DNP-BSA in Percoll density gradients. J774 cells in 10-cm dishes were incubated with ^{125}I-IgG/DNP-BSA for 90 min at 37°C in complete medium (*A*), or in medium containing 10 mM NH_4Cl (*B*), or 20 μM monensin (*C*). The cells in *B* and *C* were treated with the agents for 30 min at 37°C before the addition of IgG complexes. One dish was incubated in complete medium at 17°C for 90 min (*D*). The cells were harvested, homogenized, and the postnuclear supernatants were centrifuged in 27% Percoll as in Fig. 2. In the presence of NH_4Cl (*B*) or monensin (*C*), most of the ^{125}I-IgG complexes was found in the lysosomal fractions. In both cases, however, the low density plasma membrane/endosome peak was broader than in the control (*A*). At 17°C (*D*), no radioactivity was found in the lysosomal fractions. β-Glucuronidase activity was maximum at fractions 5–11 (peak at fraction 7; not shown).

TABLE II
Distribution of Cell-associated ^{125}I-IgG Complexes in J774 Cells Treated With Agents That Elevate Intravesicular pH

Compartment	Control	With 10 mM NH_4Cl	With 20 μM monensin
	%	%	%
Plasma membrane	22	23	24
Endosomes	20	35	35
Lysosomes	58	42	41

J774 cell monolayers were incubated in medium containing 20 μg/ml ^{125}I-IgG/DNP-BSA in the presence or absence of 10 mM NH_4Cl or 20 μM monensin. After 90 min at 37°C, the amount of plasma membrane–bound versus intracellular ligand was measured by determining the amount of ^{125}I-IgG released by subtilisin treatment in the cold (6). The cells on parallel plates were harvested by scraping, homogenized, and centrifuged in Percoll density gradients. The distribution of the ^{125}I-IgG complexes between the low density plasma membrane/endosome peak and the high density lysosome peak was obtained from gradient profiles such as those in Fig. 5. The amounts of radiolabel in fractions 5–13 (lysosomes) and in fractions 14–29 (plasma membrane/endosomes) are exposed as percentages of the total gradient radioactivity. The percentage of ^{125}I-IgG in endosomes was obtained by subtracting the percentage of subtilisin-releasable radioactivity from the percentage of radioactivity in the plasma membrane/endosome fractions.

plexes, respectively). Both types of ligand are delivered to endosomes where, unlike many other ligand-receptor systems, their dissociation from the receptor is not potentiated by the acidic endosomal pH. Although both ligands remain receptor-bound, their intracellular destinations are distinct. While monovalent ligand-FcR complexes are rapidly returned from endosomes to the cell surface, multivalent ligands are routed together with the receptor to lysosomes where both are degraded.

Since monovalent Fab and multivalent Fab-gold conjugates by definition bind to the same determinant on the receptor, the "signal" for sorting cannot depend on the mode of attachment. The main difference between the two ligands is valency, suggesting that the cells can differentiate between FcR bound to oligomeric and monomeric ligands and separate them from each other. It is also significant that Fab-gold conjugates were as efficient as multivalent IgG immune complexes (the receptor's physiological ligand) at causing the transport of receptors to lysosomes. Thus, the presence or absence of intact Fc domains is not a determining factor in directing the intracellular traffic of the receptor. It also confirms that the Fab-gold bound and entered cells via FcR. In this context, it is important to stress that the colloidal gold preparations used in these experiments did not adsorb nonspecifically to the J774 cell surface; the binding of IgG/DNP-BSA-gold or Fab-gold could be inhibited by excess 2.4G2 IgG, and the adsorption of uncomplexed DNP-BSA-gold could not be detected. However, since we could not accurately measure the stoichiometry of the Fab-gold conjugates, and since some gold particles may have been internalized as small aggregates of 3–4 (Fig. 4*B*, inset), determining the minimum degree of valency needed to trigger

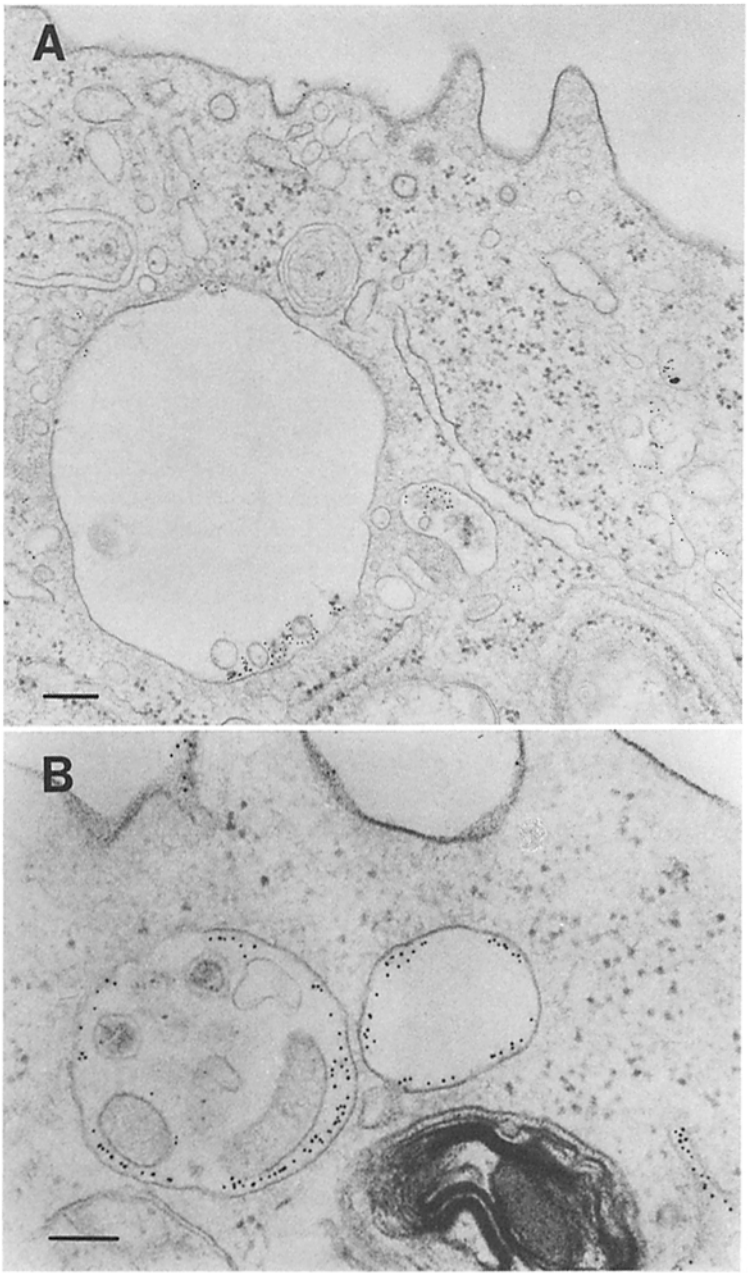

FIGURE 7. Localization of IgG/DNP-BSA-gold in endosomes at 37° and 17°C. J774 cells were incubated in colloidal gold-labeled IgG-complexes for 10 min at 37°C (*A*) or for 1 h at 17°C (*B*). As shown by Percoll gradient centrifugation (Figs. 2*B* and 6*D*), little if any ligand could be detected in high density lysosomes under these conditions. Thus, virtually all intracellular ligand was localized in endosomes. Most of the gold in the endosomes of cells incubated at 37°C was closely associated with the membranes of small vesicles in the endosome lumen (*A*). Note also the presence of gold in small (50 nm diameter) vesicles and tubules in the vicinity of the larger endosome. In cells incubated at 17°C, endosomes containing internal vesicles were much less common; when gold was observed in these structures, it was more often associated with the endosome's limiting membrane than with the membranes of the internal vesicles. Bar, 0.2 μm.

lysosomal transport will require further study using covalently stabilized Fab aggregates of defined size.

It was not possible to perform direct comparisons between IgG complexes and the corresponding monomeric IgG. The FcR is specific for binding multivalent antibody-antigen complexes and exhibits only low affinity for IgG monomer (9, 22, 23). Consequently, sufficient surface binding of labeled monomer could not be achieved to permit meaningful comparisons. To exclude the possibility that the low affinity of monomeric IgG was due to inability of the IgG to bind unless combined with its antigen, we prepared monovalent immune complexes: rabbit anti–DNP IgG complexed with either DNP-lysine or an octapeptide containing a single amino terminal DNP-lysine. Neither of these complexes bound better than monomeric rabbit ^{125}I-IgG or mouse myeloma ^{125}I-IgG2b (Ukkonen, P., and I. Mellman, unpublished results).

How might ligand valency act to control FcR transport? Since all selectivity in membrane traffic must be manifested at the level of vesicle formation or vesicle-vesicle fusion, two general possibilities must be considered. First, the binding of multivalent ligands by FcR may simply alter one or more of the kinetic characteristics of receptor transport. Multivalent ligands could, for instance, increase the rate of FcR internalization in coated pits without producing a corresponding increase in the rate of FcR recycling back to the plasma membrane. Such a situation would result in a net redistribution of receptors from the cell surface to the endosomal compartment (24) which, in turn, might increase the probability that a receptor would be transferred to lysosomes. Conversely, multivalent ligands may decrease the rate at which FcR can recycle from endosomes to the cell surface, a kinetic situation that would also result in a net redistribution of FcR to the endosomal compartment. Such a situation would occur, for example, if receptors bound to multivalent ligands were sterically limited from entering the nascent recycling vesicles that must form at the endosome membrane. A third possibility is that multivalent ligands may directly affect the rate of FcR transport from endosomes to lysosomes; e.g., they may provide a signal that increases the probability of fusion of FcR-containing endosomes (or endosome-derived transport vesicles) with lysosomes.

Another point that is illustrated by our results relates to the role of acidic intravesicular pH in the transport of ligands to lysosomes. It is generally accepted that the acidic pH in endosomes is critical to the orderly traffic of membrane, receptors, and receptor-bound ligands during endocytosis (14, 15). Low endosomal pH facilitates the disruption of many ligand-receptor complexes, permitting the return of free receptors to the cell surface and the transport of the discharged ligands to lysosomes. Lysosomal transport of many of these ligands is inhibited in cells treated with agents that elevate the pH of acidic intracellular vesicles, suggesting that the transfer of endosomal contents to lysosomes, or perhaps endosome-lysosome fusion, is directly dependent of transmembrane pH gradients (19, 20).

By studying a stable receptor-ligand complex whose dissociation is not potentiated by low pH we have been able to separate the effects of the inhibitors on receptor-ligand discharge from any direct effect on lysosomal transport. Our results show that acidic intravesicular pH is not an absolute requirement for the

transfer of internalized macromolecules from endosomes to lysosomes. Neither the transport of IgG complexes nor of fluid phase markers of endosomal content (e.g., horseradish peroxidase) was blocked in J774 cells treated with NH_4Cl. Similar results have been obtained for chorionic gonadotropin, another ligand which does not dissociate from its receptor at low pH (25), and for phagosome-lysosome fusion in macrophages (26). The role of low endosomal pH in controlling intracellular transport during endocytosis may thus be limited to facilitating the discharge of acid-sensitive ligand-receptor complexes. Conceivably, the failure of acid-dissociable ligands to reach lysosomes in the presence of the inhibitors may be an indirect result of the failure of the ligand to dissociate in endosomes. The intact receptor-ligand complexes could recycle between endosomes and the plasma membrane, as occurs for the monovalent Fab-FcR complex in NH_4Cl-treated cells (5).

Although the uptake of IgG complexes and Fab-gold is characterized by delivery of both ligand and receptor to lysosomes, it should be noted that the ligand is transferred more efficiently than the receptor. After 2 h at 37°C, 70% of the cell-associated ligand and no more than 55% of the receptor were transported to lysosomes. One explanation for this disparity is that a fraction of the receptor-bound ligand dissociates from FcR after internalization, allowing some of the receptors to recycle. Indeed, some dissociation is expected since the interaction of IgG complexes with surface FcR displays a finite (albeit pH insensitive) off-rate at 37°C (6, 22). The incomplete transfer of receptor to lysosomes may also explain why IgG complexes fail to reduce the number of surface FcR by more than 65% even after 2 h at 37°C (6).

In addition to the FcR, the intracellular traffic of several other receptors are known to be modulated by the binding of nondissociable multivalent ligands. For instance, polyvalent antibodies to the mannose 6-phosphate receptor (27), the low density lipoprotein receptor (28), the epidermal growth factor receptor (29), and the transferrin receptor (30) prevent receptor recycling and/or result in receptor transport to lysosomes. Similar observations have been made using multivalent colloidal gold conjugates of transferrin and anti–transferrin receptor antibodies (31, 32). Like the anti-FcR Fab, unconjugated monovalent transferrin usually recycles between endosomes and the plasma membrane (33). Together, these findings suggest that the valency of receptor-ligand interactions and the oligomeric structure of membrane proteins should be evaluated when considering the mechanisms that control membrane traffic.

Summary

Mouse macrophage Fc receptors specific for IgG1/IgG2b mediate the binding and pinocytic uptake of soluble IgG-containing antibody-antigen complexes. Internalization of these multivalent IgG complexes is accompanied not only by the intracellular degradation of the ligand, but also by a net decrease in the number of plasma membrane Fc receptors and an accelerated rate of receptor turnover. In contrast, internalized receptors bound to a monovalent ligand, the high affinity Fab fragment of the antireceptor mAb 2.4G2, escape degradation by rapidly recycling to the cell surface. In this paper, we have characterized the intracellular pathway involved in the endocytosis and transport of Fc receptors

in the J774 macrophage cell line. The results show that the uptake of multivalent ligands follows the normal pathway of receptor-mediated endocytosis: internalization in clathrin-coated pits and coated vesicles, delivery to endosomes, and finally to acid hydrolase–rich lysosomes. Immunoprecipitation of radiolabeled receptor from Percoll density gradients showed that endocytosis of the IgG complexes also results in the concomitant transport of the receptor to lysosomes. Although uptake of the monovalent Fab fragment had no detectable effect on intracellular receptor distribution, preparations of 2.4G2 Fab rendered multivalent by adsorption to colloidal gold were as effective as the IgG complexes at causing lysosomal accumulation of internalized receptors. Thus, it is likely that the down-regulation and degradation of Fc receptors which occurs during the endocytosis of antibody-antigen complexes is due to the transport of internalized receptors to lysosomes. Moreover, the ability of certain Fc receptor-bound ligands to interfere with receptor recycling and trigger lysosomal transport seems to depend on ligand valency rather than on the presence or absence of Fc domains on intact IgG molecules.

We wish to thank Cynthia Galloway for advice and critical reading of the manuscript; Hans Stukenbrok, Philippe Male, and Anne Beidler for assistance with electron microscopy; Steve Rosenzweig for help with HPLC; Margy Moench for artwork; Barbara Longobardi for preparing the manuscript; and Pam Ossorio for photographic work.

Received for publication 18 December 1985.

References

1. Unkeless, J. C., H. B. Fleit, and I. Mellman. 1981. Structural aspects and heterogeneity of immunoglobulin Fc receptors. *Adv. Immunol.* 31:247.
2. Mellman, I. S., and J. C. Unkeless. 1980. Purification of a functional mouse Fc receptor through the use of a monoclonal antibody. *J. Exp. Med.* 152:1048–1069.
3. Green, S. A., H. Plutner, and I. Mellman. 1985. Biosynthesis and intracellular transport of the mouse macrophage Fc receptor. *J. Biol. Chem.* 260:9867–9874.
4. Mellman, I. S., H. Plutner, R. M. Steinman, J. C. Unkeless, and Z. A. Cohn. 1983. Internalization and degradation of macrophage Fc receptors during receptor-mediated phagocytosis. *J. Cell Biol.* 96:887–895.
5. Mellman, I., H. Plutner, and P. Ukkonen. 1984. Internalization and rapid recycling of mouse macrophage Fc receptors bound to monovalent antireceptor antibody: possible role of a prelysosomal compartment. *J. Cell Biol.* 98:1163–1169.
6. Mellman, I., and H. Plutner. 1984. Internalization and degradation of macrophage Fc receptors bound to polyvalent immune complexes. *J. Cell Biol.* 98:1170–1177.
7. Unkeless, J. C. 1979. Characterization of a monoclonal antibody directed against mouse macrophage and lymphocyte Fc receptors. *J. Exp. Med.* 150:580–596.
8. Mellman, I. 1984. Membrane recycling during endocytosis. *In* Lysosomes in Biology and Pathology. Vol. 7. J. T. Dinge, R. Dean, and W. S. Sly, editors. Elsevier/North-Holland, NY. 201–229.
9. Unkeless, J. C. 1977. The presence of two Fc receptors on mouse macrophages: evidence from a variant cell line and differential trypsin sensitivity. *J. Exp. Med.* 145:931–947.
10. Baigent, C. L., and G. Miller. 1980. A colloidal gold prepared with ultrasonics. *Experientia (Basel).* 36:472–473.
11. Galloway, C. J., G. E. Dean, M. Marsh, G. Rudnick, and I. Mellman. 1983. Acidifi-

cation of macrophage and fibroblast endocytic vesicles in vitro. *Proc. Natl. Acad. Sci. USA.* 80:3334–3338.

12. Hubbard, A. L., and Z. A. Cohn. 1975. Externally disposed membrane proteins. II. Enzymatic iodination of mouse L cells. *J. Cell Biol.* 64:438–460.
13. Mellman, I. S., R. M. Steinman, J. C. Unkeless, and Z. A. Cohn. 1980. Selective iodination and polypeptide composition of pinocytic vesicles. *J. Cell Biol.* 86:712–722.
14. Brown, M. S., R. G. W. Anderson, and J. L. Goldstein. 1983. Recycling receptors: the round trip itinerary of migrant membrane proteins. *Cell.* 32:663–667.
15. Helenius, A., I. Mellman, D. Wall, and A. Hubbard. 1983. Endosomes. *Trends Biochem. Sci.* 8:245–250.
16. Steinman, R. M., I. S. Mellman, W. A. Muller, and Z. A. Cohn. 1983. Endocytosis and the recycling of plasma membrane. *J. Cell Biol.* 96:1–27.
17. McKanna, J. A., H. T. Haigler, and S. Cohen. 1979. Hormone receptor topology and dynamics: morphological analysis using ferritin-labeled epidermal growth factor. *Proc. Natl. Acad. Sci. USA.* 76:5689–5693.
18. Bjork, I., B.-A. Petersson, and J. Sjoquist. 1972. Some physicochemical properties of protein A from Staphyloccocus aureus. *Eur. J. Biochem.* 29:579–584.
19. Merion, M., and W. S. Sly. 1983. The role of intermediate vesicles in the adsorptive endocytosis and transport of ligand to lysosomes by human fibroblasts. *J. Cell Biol.* 96:644–650.
20. Harford, J., K. Bridges, G. Ashwell, and R. D. Klausner. 1983. Intracellular dissociation of receptor-bound asialoglycoproteins in cultured hepatocytes: a pH-mediated nonlysosomal event. *J. Biol. Chem.* 258:3191–3197.
21. Ohkuma, S., and P. Poole. 1978. Fluorescence probe measurement of the intralysosomal pH in living cells and the perturbation of pH by various agents. *Proc. Natl. Acad. Sci. USA.* 75:3327–3331.
22. Leslie, R. G. Q. 1980. Macrophage handling of soluble immune complexes. Ingestion and digestion of surface bound complexes at 4°, 20°, and 37°. *Eur. J. Immunol.* 10:323–333.
23. Unkeless, J. C., and H. N. Eisen. 1975. Binding of monomeric immunoglobulins to Fc receptors of mouse macrophages. *J. Exp. Med.* 142:1520–1533.
24. Schwartz, A. L., S. E. Fridovich, and H. F. Lodish. 1982. Kinetics of internalization and recycling of the asialoglycoprotein receptor in a hepatoma cell line. *J. Biol. Chem.* 257:4230–4237.
25. Ascoli, M. 1984. Lysosomal accumulation of the hormone-receptor complex during receptor-mediated endocytosis of human choriogonadotropin. *J. Cell Biol.* 99:1242–1250.
26. Kielian, M. C., and Z. A. Cohn. 1982. Intralysosomal accumulation of polyanions. II. Polyanion internalization and its influence on lysosomal pH and membrane fluidity. *J. Cell Biol.* 93:875–882.
27. von Figura, K., V. Gieselmann, and A. Hasilik. 1984. Antibody to mannose 6-phosphate specific receptor induces receptor deficiency in human fibroblasts. *EMBO (Eur. Mol. Biol. Organ.) J.* 3:1281–1282.
28. Anderson, R. G. W., M. S. Brown, U. Beisiegel, and J. L. Goldstein. 1982. Surface distribution and recycling of the low density lipoprotein receptor as visualized with anti-receptor antibodies. *J. Cell Biol.* 93:523.
29. Schreiber, A. B., T. A. Liberman, I. Lax, Y. Yarden, and J. Schlessinger. 1983. Biological role of epidermal growth factor receptor clustering. Investigation with monoclonal anti-receptor antibodies. *J. Biol. Chem.* 258:846–854.
30. Ekblom, P., I. Thesleff, V.-P. Lehto, and I. Virtanen. 1983. Distribution of the

transferrin receptor in normal human fibroblasts and fibrosarcoma cells. *Int. J. Cancer.* 31:111–120.

31. Hopkins, C. R., and I. S. Trowbridge. 1983. Internalization and processing of transferrin and the transferrin receptor in human carcinoma A431 cells. *J. Cell Biol.* 97:508–517.
32. Willingham, M. C., J. A. Hanover, R. B. Dickson, and I. Pastan. 1984. Morphologic characterization of the pathway of transferrin endocytosis and recycling in human KB cells. *Proc. Natl. Acad. Sci. USA.* 81:175–179.
33. van Renswoude, J., K. Bridges, J. Harford, and R. D. Klausner. 1982. Receptor-mediated endocytosis of transferrin and the uptake of Fe in K562 cells: identification of a non-lysosomal acidic compartment. *Proc. Natl. Acad. Sci. USA.* 79:6186–6190.